TISSUE ENGINEERING: Part A
Volume 23, Numbers 5 and 6, 2017

DOI: 10.1089/ten.tea.2016.0263

termis
Tissue Engineering
& Regenerative Medicine
International Society

ORIGINAL ARTICLE

Injectable Shape-Memorizing Three-Dimensional Hyaluronic Acid Cryogels for Skin Sculpting and Soft Tissue Reconstruction

Liying Cheng, MD, PhD,[1,2,*] Kai Ji, MD, PhD,[1,3,*] Ting-Yu Shih, PhD,[4,5] Anthony Haddad, MD,[1] Giorgio Giatsidis, MD,[1] David J. Mooney, PhD,[4,5] Dennis P. Orgill, MD, PhD,[1] and Christoph S. Nabzdyk, MD[1,6]

Introduction: Hyaluronic acid (HA)-based fillers are used for various cosmetic procedures. However, due to filler migration and degradation, reinjections of the fillers are often required. Methacrylated HA (MA-HA) can be made into injectable shape-memorizing fillers (three-dimensional [3D] MA-HA) aimed to address these issues. In this study, shape retention, firmness, and biocompatibility of 3D MA-HA injected subcutaneously in mice were evaluated.

Materials and Methods: Fifteen mice, each receiving two subcutaneous injections in their back, were divided into four groups receiving HA, MA-HA, 3D MA-HA, or saline, respectively. Digital imaging, scanning electron microscope (SEM) and *in vivo* imaging system (IVIS), durometry, and histology were utilized to evaluate *in vitro*/vivo degradation and migration, material firmness, and the angiogenic (CD31) and immunogenic (CD45) response of the host tissue toward the injected materials.

Results: Digital imaging, SEM, and IVIS revealed that 3D MA-HA fillers maintained their predetermined shape for at least 30 days *in vitro* and *in vivo*. Little volume effects were noted in the saline and other control groups. There were no differences in skin firmness between the groups or over time. Histology showed intact skin architecture in all groups. Three-dimensional MA-HA maintained its macroporous structure with significant angiogenesis at the 3D MA-HA/skin interfaces and throughout the 3D MA-HA. There was no significant inflammatory response to any of the injected materials.

Conclusion: 3D MA-HA showed remarkable tissue compatibility, compliance, and shape predictability, as well as retention, and thus might be suitable for various skin sculpting and soft tissue reconstruction purposes.

Keywords: hyaluronic acid, filler, shape-memorizing, injectable, skin sculpturing, soft tissue reconstruction, scaffold, regeneration, plastic surgery

Introduction

With an increasing understanding of the aging process and the rapidly growing interest in minimally invasive treatments, injectable facial fillers have become a major treatment modality for the rejuvenation of the aging face.[1] Hyaluronic acid (HA) fillers are some of the most popular dermal filler agents,[2,3] which when injected into and below the dermis can provide cosmetic volume improvements.[2,4,5] However, these volume effects will diminish soon after injection.[6,7] Filler migration and (non)-enzymatic HA degradation can further lead to progressive volume loss and shape deformity at the site of injection requiring reinjection.[8] Subsequent fibroblast activation and neocollagenesis only result in partial HA filler engraftment into the surrounding tissue.[9–11] Due to filler migration, degradation,

[1]Tissue Engineering and Wound Healing Laboratory, Division of Plastic Surgery, Brigham and Women's Hospital, Harvard Medical School, Boston, Massachusetts.
[2]Department of Plastic and Reconstructive Surgery, Shanghai Ninth People's Hospital, Shanghai Jiao Tong University, School of Medicine, Shanghai, China.
[3]Department of Plastic Surgery, China–Japan Friendship Hospital, Beijing, China.
[4]Wyss Institute for Biologically Inspired Engineering, Harvard University, Boston, Massachusetts.
[5]John A. Paulson School of Engineering and Applied Sciences, Harvard University, Cambridge, Massachusetts.
[6]Department of Anesthesiology, Perioperative and Pain Medicine, Brigham and Women's Hospital, Harvard Medical School, Boston, Massachusetts.
*These authors contributed equally.

and lack of filler engraftment into the surrounding tissue, reinjection of the fillers is often required. Thus, there is a need for a more durable, shaped-defined HA filler with improved tissue engraftment properties.

One limiting factor for HA filler is particle size. Existing HA filler particle diameters range between 300 and 700 μm.[4] As fillers are typically injected, particle diameters thus far could not be increased to any size. HA filler is further characterized by HA concentration and degree of HA cross-linking.[4,5,9,12] Filler migration has been only partially addressed by increasing the viscosity of the injected solution. It is of great interest for plastic surgeons to be provided with an injectable filler compound that can predictably fill volume defects and will remain at the injection site for long-lasting results.

Such long-lasting and injectable fillers should be nonimmunogenic, nontoxic, possess favorable mechanical properties, and act as cellular scaffolds to promote integration into the surrounding tissues. In recent years, the process of cryogelation has been described. These cryogels could meet all the requirements above and thus address filler migration, degradation, and cellularization.[13–15] Once injected, cryogels can restore their original shape and elicit considerable volume effect. Furthermore, their macroporous ultrastructure promotes oxygen permeation and cellular ingrowth.[13] The process to produce these cryogels is highly customizable, in that different polymers such as alginate, HA, or others can be used and different cryogel sizes and shapes can be created. Rate of degradation and firmness can also be adjusted. This study evaluates injectable HA cryogels (three-dimensional [3D] MA-HA, diameter of up to 5 mm) regarding their shape memory capabilities, degradation, firmness, and tissue compatibility.

Materials and Methods

Materials

HA (Bacterial, strep, Pyogenes, 1.38 MDa MW) was purchased from Lifecore Biomedical Company; phosphate-buffered saline (PBS), N,N-dimethylformamide (DMF), glycidyl methacrylate (GM), triethylamine (TEA), acetone, N,N,N′,N′-tetramethylethylenediamine (TEMED), ammonium persulfate (APS), 2-morpholinoethanesulfonic acid (MES buffer), N-hydroxysuccinimide (NHS), 1-ethyl-3-(3-dimethylaminopropyl)-carbodiimide hydrochloride (EDC), and hexamethyldisilazane (HMDS) were purchased from Sigma-Aldrich. Cyanine-7 amine (Cy7-amine) was purchased from Lumiprobe Corp. A customized Teflon mold was supplied by Harvard University. Proteinase K (Roche Diagnostics Corp.), DAB Substrate Chromogen System (Dako North America, Inc.), CD31 (BD Pharmingen™), and CD45 (BD Biosciences) were used in this study.

HA methacrylation

Methacrylated HA (MA-HA) was prepared by reacting HA with DMF, TEA, and GM. HA (1 g) was dissolved in 200 mL PBS. Sixty-seven milliliters of DMF was slowly added to the solution.[13] This step could generate heat, and the solution was then cooled down in ice water to room temperature (RT) before GM (13.3 g) and TEA (6.7 g) were added to the mixture. The solution was then stirred at RT for 7 days. The mixture was washed, precipitated in acetone, filtered, and dried in a vacuum chamber overnight at RT, yielding the solid MA-HA polymer. MA-HA was then purified and dialyzed for 3 days, placed in liquid nitrogen to freeze down, and subsequently dried using a lyophilizer (4 days) (Supplementary Fig. S1A, B; Supplementary Data are available online at www.liebertpub.com/tea).

Three-dimensional MA-HA cryogel fabrication

Three-dimensional MA-HA was synthesized by redox-induced free-radical polymerization of MA-HA in water. MA-HA solution (2.5% [w/v]) was prepared by dissolving the MA-HA in deionized water. Three-dimensional MA-HA cryogels were synthesized by mixing 500 μL of MA-HA solution (2.5% [w/v]) with 20 μL TEMED (70 mg/mL) to make a prepolymer solution in an Eppendorf tube, which was then placed in a 4°C fridge for at least 10 min until use. Ten microliters of APS (137 mg/mL) was added to the MA-HA solution. The APS solution was precooled to 4°C to decrease the rate of polymerization before freezing. The mixed solution was then vortexed. Once the APS was added to the prepolymer solution, the solution was quickly poured into a precooled (−20°C) Teflon mold and incubated overnight (Fig. 1). The solution froze within a minute, while a witness solution stored at 4°C remained unpolymerized for at least 20 min. After a complete incubation period of 17 h, the gels were warmed to RT to remove ice crystals and washed with deionized water (Supplementary Fig. S1C).

In vitro *degradation of 3D MA-HA cryogel*

Heart-shaped 3D MA-HA cryogels were manufactured as above and according to previously described cryogel fabrication protocols (Supplementary Fig. S1).[13] Structural analysis of the

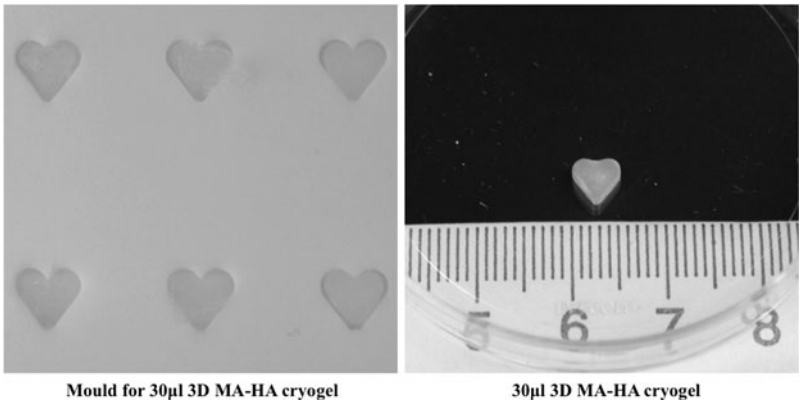

FIG. 1. *Left*: heart-shaped Teflon molds for 30 μL 3D MA-HA cryogel. *Right*: 30 μL 3D MA-HA before injection into the back of a mouse. 3D MA-HA, three-dimensional methacrylated hyaluronic acid.

cryogels was performed to evaluate *in vitro* degradation using a scanning electron microscope (SEM) (Ultra Plus Electron Microscopy). Serial SEM images of 3D MA-HA incubated in normal saline at 37°C on an orbital shaker for 0, 7, 14, and 28 days were obtained. Each time point had 4 samples reserved for scanning. After the incubation period, cryogels were rinsed in PBS and dehydrated in increasing concentration of ethanol (30%, 50%, 70%, 90%, and 100%) for 20 min each, soaked in HMDS for 10 min, followed by drying in vacuum desiccators. The dried samples were then sectioned and coated with gold for SEM scanning at 3.0 kV and 1000× of magnification. The pore diameter was measured by averaging the values of the largest and the smallest axis of the pore. The average pore size of cryogels was calculated by averaging the gel pore diameters observed by SEM.

In vivo *imaging system imaging*

Location and degradation of the injected fillers were indirectly visualized by noninvasive fluorescence *in vivo* imaging system (IVIS). Three-dimensional MA-HA cryogel scaffolds, regular HA solution, MA-HA solution, and saline were first labeled using Cy7-amine and then sterilized.

Cy7-amine was covalently conjugated to HA, MA-HA, and the 3D MA-HA cryogel. Cy7-amine (0.392 mg) was diluted in 20 mL MES buffer in which EDC (130 mg) and NHS (60.4 mg) were added to make the labeling mixture solution. For 3D MA-HA cryogel-Cy7, 10 cryogels were placed in a Petri dish with 10 mL (1 mL/gel) of labeling mixture solution and shaken gently in RT for 3 h. For HA-Cy7 solution and MA-HA-Cy7 solution, HA solution and MA-HA solution (100 mg per 20 mL MES buffer) were placed into the labeling mixture solution and shaken gently in RT for 3 h, and then dialyzed for 4 days, followed by sterile filtration and lyophilization. Saline-Cy7 solution was made by diluting Cy7-amine (0.392 mg) into saline (20 mL).

Eight female C57 BL/6J mice (Jackson Laboratory), 4–6 weeks of age, were divided into four groups: 3D MA-HA cryogel-Cy7 ($n=4$), HA-Cy7 solution ($n=4$), MA-HA-Cy7 solution ($n=4$), and saline-Cy7 ($n=4$) (Fig. 2). The backs of the mice were shaved and dehaired using depilatory cream under general anesthesia according to the approved IACUC protocol. Thirty microliters of 3D MA-HA-Cy7, HA-Cy7 solution (2.5%), MA-HA-Cy7 solution (2.5%), or saline-Cy7 was then injected subcutaneously together with 200 μL saline as carrier solution in the dorsum of the mice using a 16G angiocath catheter.

Optical bioluminescence images of mice were obtained using an IVIS live animal imaging system (Caliper Life Sciences). Images were taken on days 0, 6, 12, 18, 24, and 30 to allow a longitudinal analysis. High-sensitivity fluorescence imaging was quantified by creation of polygonal regions of interest.

Animal injection for in vivo *evaluation*

The same cryogels used for *in vitro* degradation were manufactured according to cryogel fabrication protocols for animal injection. Female C57 BL/6J mice ($n=15$; The Jackson Laboratory), 4–6 week of age, were divided into four groups ($n=4$–11), saline ($n=4$), HA ($n=8$), MA-HA ($n=7$), and 3D MA-HA ($n=11$) (Fig. 2). Same injection techniques were applied as in the method described in the *In Vivo* imaging system imaging section. Serial imaging on days 0, 6, 12, 18, 24, and 30 was carried out. Animals were sacrificed on day 30. A single investigator harvested full-thickness skin biopsies from the injected areas with a 10-mm biopsy punch. All specimens underwent histologic and morphometric analysis.

Skin firmness evaluation by durometry

A highly sensitive digital 00–000 Shore durometer was used to evaluate the firmness of the skin before and after injection of the respective compounds. This methodology has been widely used to evaluate skin firmness both in patients and in experimental animal models.[16,17] This technique is noninvasive and therefore no significant distress and technical complications for the animals were experienced. Time points were days 1, 3, 6, 12, 18, 24, and 30. Three measurements per time point and treatment group were obtained and values were averaged. One-way analysis of variance (ANOVA) was performed for statistical analysis.

Histologic evaluation of tissue response to injected cryogels

Histology (hematoxylin and eosin) and immunohistochemistry (endothelial cell marker platelet endothelial cell adhesion molecule-1 CD31, pan-leukocyte marker CD45) of samples were performed according to previously described standard protocols.[18,19] Images were acquired using a Nikon E200 microscope (Nikon Corp.). Density of blood vessels and density of $CD45^+$ inflammatory cells were quantified according to previously established methods.[18,19] For each slide and staining, three high-power fields were evaluated by two blinded reviewers with experience in skin histology and trained in the specific methods used in this study.

Statistical analysis

All the results are expressed as the mean ± SD in text and figures. One-way ANOVA (Win-STAT; R. Fitch Software) with

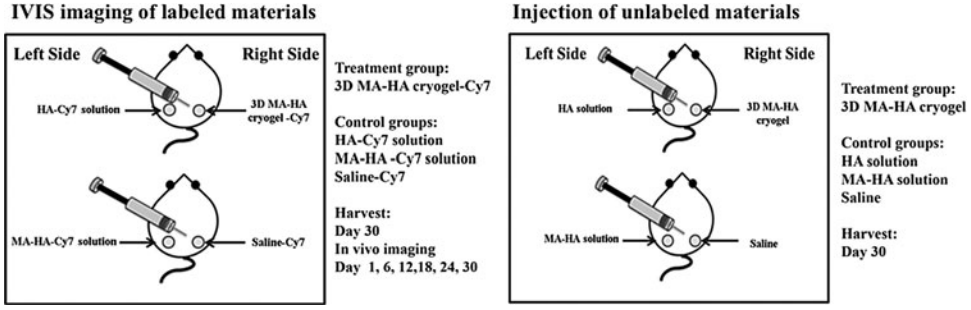

FIG. 2. Study design. *Left*: injection of 3D MA-HA cryogel-Cy7, HA-Cy7 solution, MA-HA-Cy7 solution, and saline-Cy7 in the dorsum of mice. *Right*: respective injections of unlabeled of saline, HA, MA-HA, or 3D MA-HA.

Tukey's *post hoc* correction was used to determine the significance of differences for quantitative immunohistochemistry. A value of $p < 0.05$ was considered statistically significant.

Results

Three-dimensional MA-HA cryogel fabrication

To prepare HA amenable to cryogelation, pendant methacryloyl groups were first introduced into the HA main chains (Supplementary Fig. S1A, B). By the process of cryogelation at −20°C and utilizing a free-radical cross-linking mechanism, MA-HA was used to generate macroporous 3D MA-HA cryogels. During cryotropic gelation, most of the solvent (water) was frozen, and the dissolved solutes (macromonomers and initiator system) were concentrated in small semifrozen regions called nonfrozen liquid microphase, in which the free-radical cryopolymerization of MA-HA occurred (Supplementary Fig. S1C). After complete polymerization, 3D MA-HA cryogels were incubated at RT and washed with deionized water to remove unreacted polymeric precursors. The ice crystals melted, leaving behind a network of interconnected pores (Fig. 3); 2.5% MA-HA solutions and 2.5% HA solutions were prepared at RT, which were designated as conventional, noncross-linked control group agents.

In vitro *degradation of 3D MA-HA*

SEM imaging of 3D MA-HA revealed the aforementioned highly interconnected pore structure with the average pore size of 15–62 μm (in the range of 12–167 μm) with the median value of 32.2 μm. Serial SEM imaging showed largely unchanged ultrastructure of interconnected pores on days 0, 7, 14, 21, and 28, respectively (Fig. 3). Three-dimensional MA-HA maintained its porous ultrastructure for at least 28 days of *in vitro* incubation in normal saline at 37°C on an orbital shaker.

Injectability and shape memory of cryogels

A unique feature of these cryogels is their shape memory. Heart-shaped 3D MA-HA cryogels (Fig. 1) were suspended in 0.2 mL of saline and successfully passed through a 16G needle (Supplementary Movie S1). The large volumetric change of the macroporous gels was presumably caused by a reversible collapse of the pores. When the sheer force was discontinued after injection, deformed gels rapidly returned to their original nondeformed configuration, as surrounding water was reabsorbed into the gels (Supplementary Movie S1).

When the 3D MA-HA scaffolds were dehydrated, they collapsed and assumed irregular shapes. Upon rehydration, they quickly regained their original shapes (Supplementary Movie S2).

Three-dimensional MA-HA morphology and biocompatibility in vivo

Sterile heart-shaped 3D MA-HA cryogels (Fig. 1) were successfully injected subcutaneously in the back of mice with 200 μL saline as carrier solution using a 16G angiocath catheter (Fig. 4). The deformed gels rapidly regained their original shapes by reabsorbing the surrounding water. During the 30 days of observation, 3D MA-HA maintained its predetermined shape *in vivo* (Fig. 4). This shape was still clearly visible on day 30 and after explantation. Only the 3D MA-HA group demonstrated a robust and lasting volume effect after a single injection of only 30 μL of compound. Moreover, 3D MA-HA was still located at the original injection site without diffusion or migration. No adverse events such as bleeding, infection, inflammation, or allergic reactions were noted at any time point. No capsule formation was found after 30 days.

Longitudinal IVIS imaging for in vivo *3D-MA-HA localization after subcutaneous injection in mice*

To further evaluate the degradation and diffusion of the 3D-MA-HA cryogel, IVIS was performed. Cy7-labeled saline, HA, MA-HA solution, and 3D MA-HA cryogel were injected in the dorsum of mice, and serial imaging on days 0, 6, 18, and 30 was performed (Fig. 5). All groups showed fluorescence signals instantly after injection, which indicated successful injection and *in vivo* localization of the injected compounds. In the saline-Cy7 injection group, fluorescence signal could not be detected on day 6. In the HA-Cy7 and the MA-HA-Cy7 groups, the fluorescence signal disappeared by day 18. In contrast, the signal site of

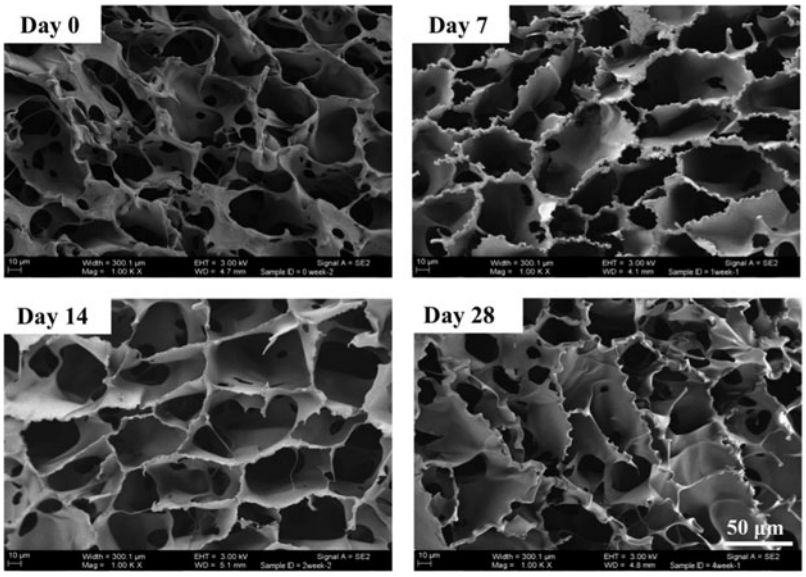

FIG. 3. Scanning electron microscope imaging of 3D MA-HA incubated in normal saline at 37°C on an orbital shaker for up to 28 days. Imaging revealed largely unchanged ultrastructure of interconnected pores.

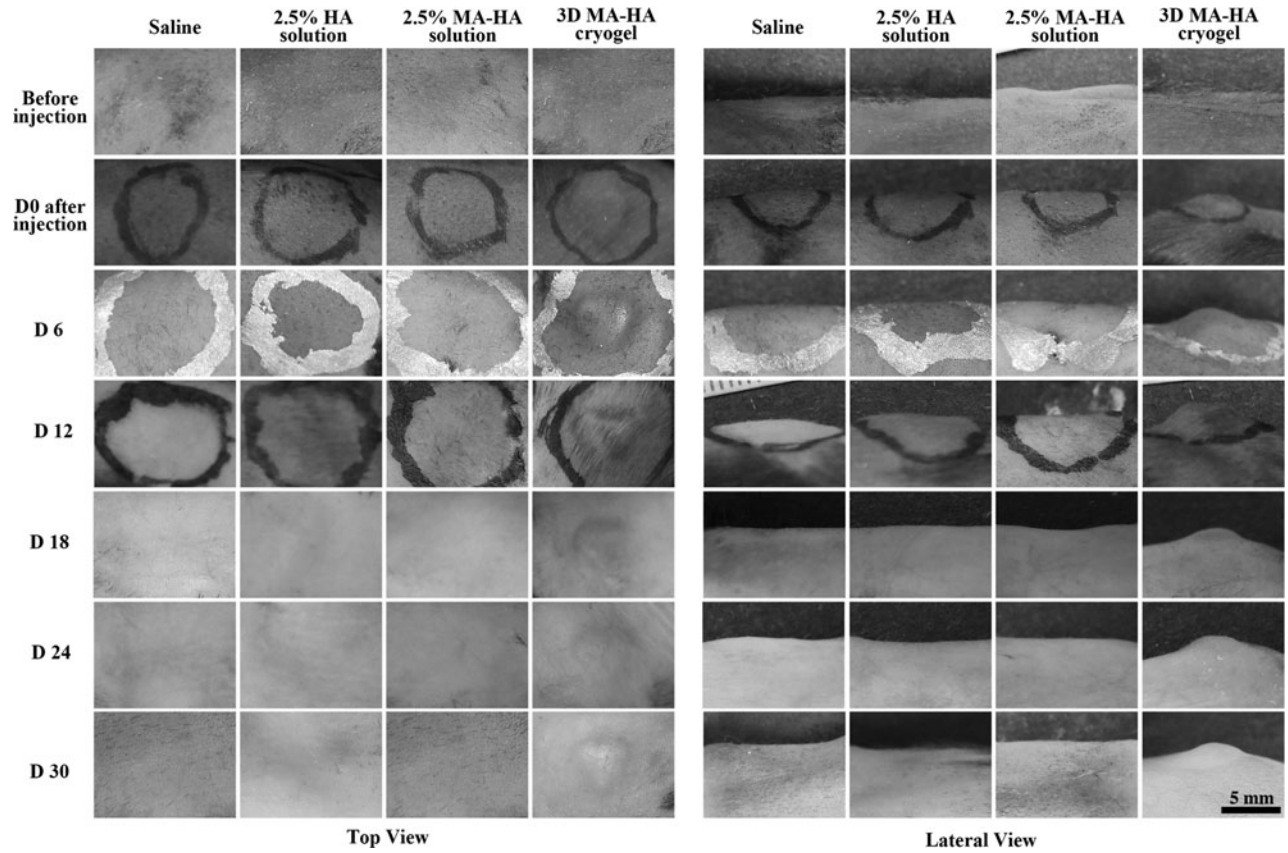

FIG. 4. Photo panels of the four treatment groups from the top (*left panel*) and from a lateral view (*right panel*). Only 3D MA-HA elicited a predictable and lasting volumetric effect while maintaining the predetermined heart shape for at least 30 days. No signs of inflammation or infection were noted.

3D MA-HA-Cy7 emitted a robust fluorescence signal for at least 30 days after injection in the dorsum of mice (Fig. 5). In addition, 3D MA-HA-Cy7 remained exactly at its injection site for at least 30 days without obvious signs of significant degradation or migration.

Evaluation of skin firmness by durometry

Skin firmness at the injection sites was measured using a highly sensitive OOO-Durometer. The average values showed no significant differences between the treatment groups or within a group over time (Fig. 6). This is an important finding as the goal is to develop an injectable compound that not only provides a significant volume effect but also maintain firmness similar to the surrounding skin.

Histological analysis of mouse skin injected with 3D MA-HA

Histological analysis revealed intact architecture of subcutaneous tissue above and below the panniculus carnosus in all animals 30 days after treatment (Fig. 7). No inflammation was observed in subcutaneous tissues either above or below the panniculus carnosus in any group. Three-dimensional-MA-

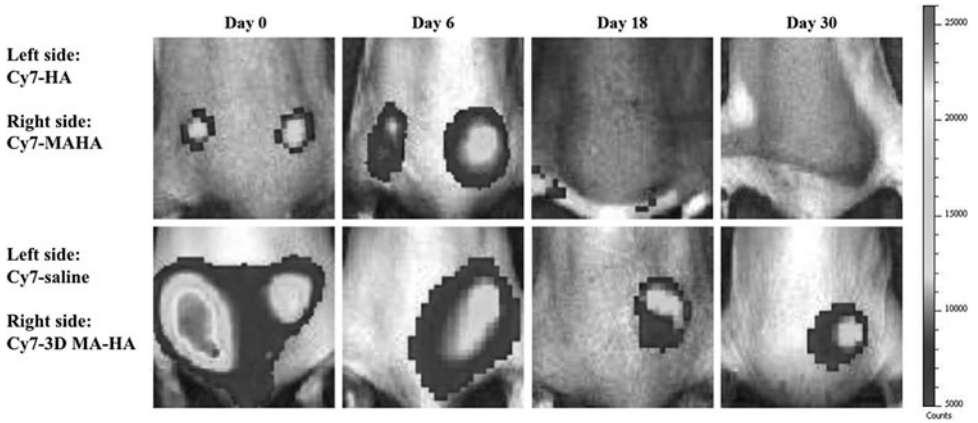

FIG. 5. Serial *in vivo* fluorescence imaging of mice locally injected with equal volumes of Cy7-containing saline, Cy7-labeled HA, MA-HA, or 3D MA-HA. Only 3D MA-HA-Cy7 showed persistent fluorescence signals for at least 30 days. Of note, there was no migration of the fluorescence 3D MA-HA-Cy7 signal, suggesting that 3D MA-HA-Cy7 remained at the initial injection site. Skin sites injected with Cy7-containing saline or Cy7-labeled HA, MAHA showed no fluorescence by day 30.

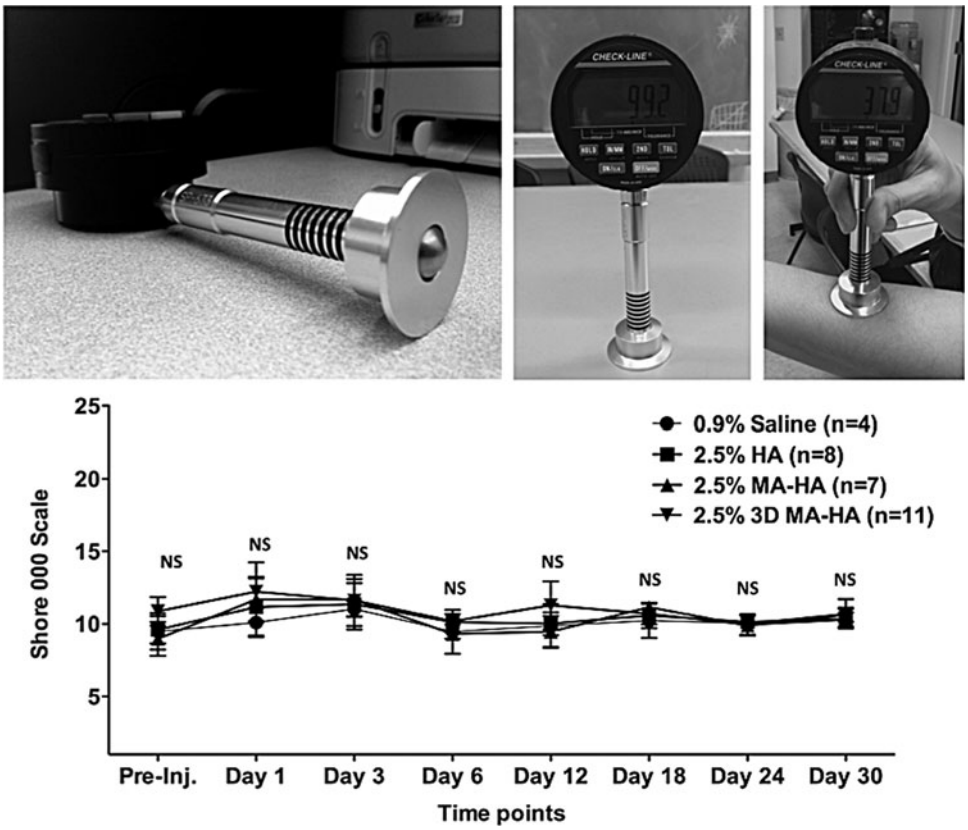

FIG. 6. Durometry was used to detect skin firmness. The digital 00–000 Shore durometer scale ranges from 0 to 100. *Top*: durometer hardness testing temporarily deforms the tested material by impinging the indenting pin on the tested surface. The relative movement of the durometer's indenting pin is measured and converted into a hardness value. *Bottom*: no significant differences were noted between any of the treatment groups at any given time point.

HA matrices were clearly visible in the subcutaneous tissue and cellularization of 3D MA-HA occurred homogeneously and throughout the cryogels. This result indicated that 3D-MA-HA maintained its macroporous ultrastructure 30 days after injection and showed signs of cellularization (Fig. 7).

Evaluation of angiogenesis (CD31) and immune cell infiltration (CD45) in response to subcutaneous filler injection

No statistically significant differences were found in the density of $CD31^+$ blood vessels in the subcutaneous tissue above the panniculus carnosus at the injection site among different groups (Fig. 8). In contrast, the subcutaneous tissue below the panniculus carnosus at the injection site revealed a significantly higher $CD31^+$ blood vessel density in the 3D MA-HA group (Fig. 8) when compared with controls. Moreover, angiogenesis was noted not only at the host tissue to scaffold interface but also throughout the injected 3D MA-HA. This result suggests that the porous structure and chemical composition of 3D MA-HA promoted host tissue ingrowth and possible engraftment.

There was no significant difference in $CD45^+$ cell counts in either layer (subcutaneous tissue above or below the panniculus carnosus) and across the respective groups on

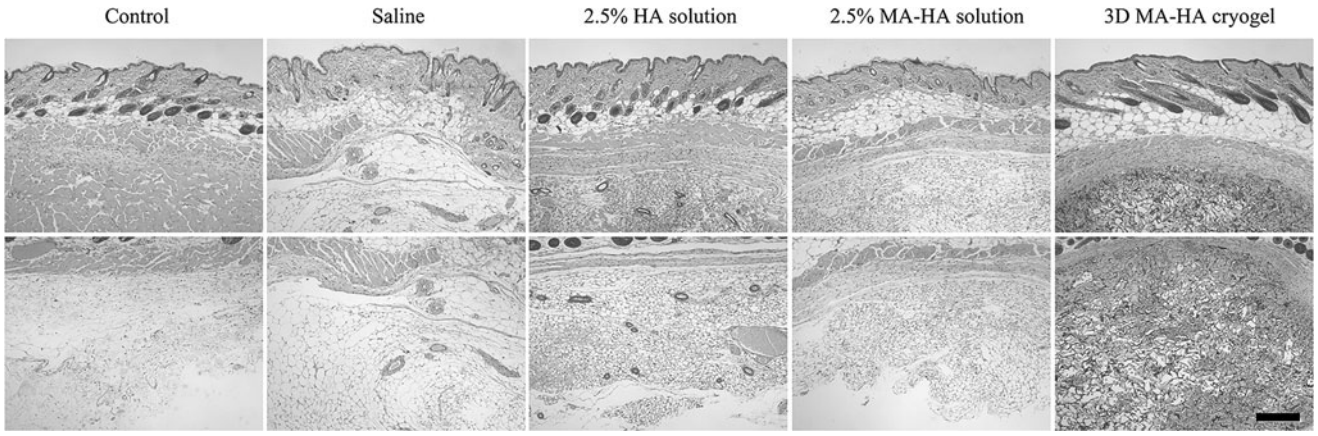

FIG. 7. Hematoxylin and eosin staining of treated mouse skin after 30 days. Three-dimensional MA-HA maintained its macroporous ultrastructure 30 days after injection and showed signs of cellularization. The overall skin architecture was not adversely altered by either treatment. *Upper panel*: subcutaneous tissues above the panniculus carnosus; *bottom panel*: subcutaneous tissues below the panniculus carnosus. Scale bar represents 400 μm.

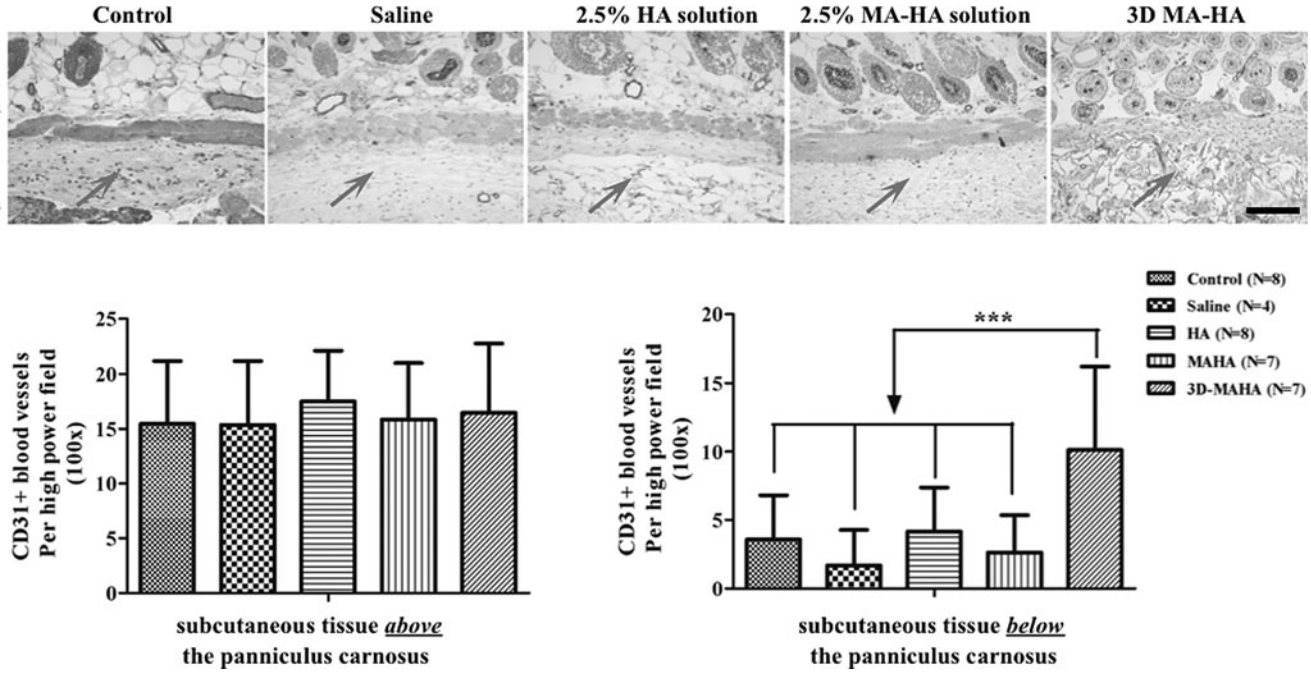

FIG. 8. CD31 staining of dorsal mouse skin 30 days after injection with saline, HA, MA-HA, or 3D MA-HA. A significantly higher CD31 count was noted in the layer below the panniculus carnosus of mice at the site of 3D MA-HA injection on day 30 when compared with the control groups. On day 30, there were no differences in CD31 counts in the layer above the panniculus carnosus at the site of injection across the groups. *Arrow* represents injection area. Scale bar represents 200 μm. * represents $p < 0.05$.

day 30 (Fig. 9). This result suggests that neither saline, HA, and MA-HA nor 3D MA-HA induced tissue inflammation or immune cell infiltration in the skin that was present by day 30 after injection.

Discussion

Success of modern skin filler therapy is limited by filler agent degradation, migration, and lack of incorporation. This study evaluated 3D MA-HA as a filler material aimed to address these three major issues. The cryogelation process yielded a scaffold with a highly porous interconnected and tightly cross-linked internal microarchitecture. This caused the cryogels to collapse when experiencing sheer stress during injection and to rapidly resume their predetermined shape once placed into the body without mechanical fracture. The *in vitro* data illustrated that 3D MA-HA degraded very slowly at body temperature in an aqueous phase as evidenced by the unchanged porous ultrastructure on SEM imaging on day 28 (Fig. 3). This further demonstrated that 3D MA-HA consisted of a stable porous system that did not significantly swell in a wet state. No apparent weakening of the interconnected pores occurred.

This study also revealed that 3D MA-HA of a defined shape (heart shape, with diameter up to 5 mm) could be injected subcutaneously through a conventional 16G catheter syringe in the dorsum of mice. After the injection, 3D MA-HA quickly regained the original shape (Supplementary Movie S2). Three-dimensional MA-HA resided at the site of injection and provided lasting volume-enhancing effects for at least 30 days. None of the control groups provide any comparable effects. Even on day 30, the predetermined heart shape could clearly be

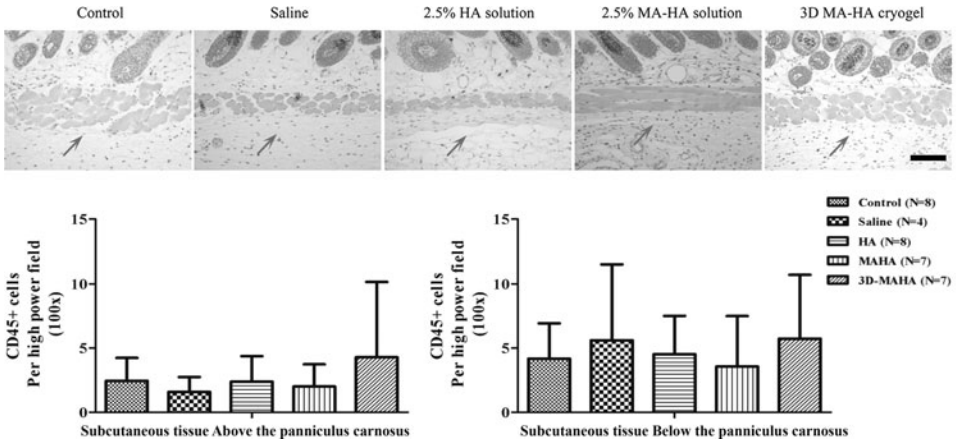

FIG. 9. CD45 staining of dorsal mouse skin 30 days after injection with saline, HA, MA-HA, or 3D MA-HA. No differences in CD45 counts were noted between the different treatment groups on day 30 after injection. *Arrow* represents injection area. Scale bar represents 200 μm. *Bottom panels:* no statistically significant differences were found between the different treatment groups.

seen at the injection site (Fig. 4) and after explantation (Supplementary Fig. S2). The shape restoration of 3D MA-HA cryogels in the subcutaneous layer did not cause extra tension on the skin, local inflammation, or edema.

Filler therapy should reproduce firmness and overall texture similar to the untreated surrounding skin. Durometry yields precise data about tissue firmness and can detect subtle differences in skin texture.[20–25] In this study, durometry revealed that skin injected with 3D MA-HA had similar firmness as the control groups and no changes over the course of 30 days were noted (Fig. 6).

As conventional HA filling agents typically consist of viscous HA, filler migration and insufficient incorporation are common. In contrast to the control groups, significant cellularization and angiogenesis ($CD31^+$ staining) were detected at the interface of 3D MA-HA and the host tissue as well as throughout 3D MA-HA itself. This tissue engraftment might be a result of the 3D MA-HA unique porous ultrastructure that allowed for the passage of oxygen and nutrients, as well as cell migration and cell–cell interaction. SEM imaging of 3D MA-HA showed an average pore size between 15 and 62 μm with a median value of 32.2 μm. It has been previously shown that the macroporous scaffolds used for *in vivo* tissue regeneration had better biological activity when their pore size located in a certain range of 20–150.5 μm.[26,27]

Filler should not evoke a significant inflammatory response as this could result in foreign body and granuloma formation, nor should other potentially catastrophic complications such as tissue necrosis be a concern.[28–32] Our data did not reveal any significant differences in immune cell infiltration between the groups on day 30. While this is encouraging, one limitation of the study is that no early time point analysis was performed to assess for potential early inflammatory reactions in response to filler injection. That being said, there was no clinical evidence that 3D MA-HA caused skin irritation, bleeding, or other adverse skin reaction at any time point.

One of the most important complications of commercial HA filler injection is vascular embolism, which may result in tissue/organ necrosis and even blindness or stroke. This is because the particle size of various HA fillers is close to the diameter of the blood vessels present in subcutaneous layers. These filler particles may inadvertently enter these blood vessels causing partial or complete vessel occlusion. Plastic surgeons nowadays are working on improved injection techniques and rescue solutions once embolism occurred.[33–35] Our injected 3D MA-HA cryogel had a diameter of 5 mm, which is far larger than the diameter of subcutaneous blood vessels, thus minimizing the risk of inadvertent blood vessel embolization.

In summary, 3D MA-HA demonstrated key features that address some of the major limitations of current conventional filler therapy.

Conclusions

Injectable 3D MA-HA cryogels of at least 5 mm in diameter could be successfully deployed through a 16G catheter into the subcutaneous compartment of C57 BL/6J mice. Three-dimensional MA-HA regained its original shape, which it maintained for at least 30 days without any signs of adverse reaction to the surrounding. Three-dimensional MA-HA injection did not affect skin firmness, nor did it cause a significant inflammatory response over the studied time. Three-dimensional MA-HA did appear to become cellularized, including widespread neoangiogenesis. Therefore, it is concluded that 3D MA-HA may be a new candidate substrate for skin sculpting and soft tissue reconstruction. To further confirm its clinical applicability, additional studies should be carried out to characterize its long-term outcomes, biodegradation rate, inflammatory reaction, and systemic toxicology.

Acknowledgments

Dr. Christoph S. Nabzdyk is a recipient of a pilot research grant given to Brigham and Women's Hospital by the Plastic Surgery Foundation, which is related to this project. The work was further supported by NIH T-32 grant 5T32HL007734-20 awarded to Dr. Frank W. LoGerfo, MD. The authors also thank the Gillian Reny Stepping Strong Fund for the generous donation that helped accomplish this work.

Disclosure Statement

No competing financial interests exist.

References

1. Attenello, N.H., and Maas, C.S. Injectable fillers: review of material and properties. Facial Plast Surg **31,** 29, 2015.
2. Carruthers, J., Carruthers, A., and Humphrey, S. Introduction to fillers. Plast Reconstr Surg **136,** 120S, 2015.
3. Lupo, M.P. Hyaluronic acid fillers in facial rejuvenation. Semin Cutan Med Surg **25,** 122, 2006.
4. Kablik, J., Monheit, G.D., Yu, L., Chang, G., and Gershkovich, J. Comparative physical properties of hyaluronic acid dermal fillers. Dermatol Surg **35,** Suppl 1: 302, 2009.
5. Sundaram, H., and Cassuto, D. Biophysical characteristics of hyaluronic acid soft-tissue fillers and their relevance to aesthetic applications. Plast Reconstr Surg **132,** 5S, 2013.
6. De Boulle, K. Management of complications after implantation of fillers. J Cosmet Dermatol **3,** 2, 2004.
7. Mummert, M.E. Immunologic roles of hyaluronan. Immunol Res **31,** 189, 2005.
8. Fakhari, A., and Berkland, C. Applications and emerging trends of hyaluronic acid in tissue engineering, as a dermal filler and in osteoarthritis treatment. Acta Biomater **9,** 7081, 2013.
9. Bertossi, D., Sbarbati, A., Cerini, R., Barillari, M., Favero, V., Picozzi, V., Ruzzenente, O., Salvagno, G., Guidi, G.C., and Nocini, P. Hyaluronic acid: in vitro and in vivo analysis, biochemical properties and histological and morphological evaluation of injected filler. Eur J Dermatol **23,** 449, 2013.
10. Wang, F., Garza, L.A., Kang, S., Varani, J., Orringer, J.S., Fisher, G.J., and Voorhees, J.J. In vivo stimulation of a de novo collagen production caused by cross-linked hyaluronic acid dermal filler injections in photodamaged human skin. Arch Dermatol **143,** 155, 2007.
11. Turlier, V., Delalleau, A., Casas, C., Rouquier, A., Bianchi, P., Alvarez, S., Josse, G., Briant, A., Dahan, S., Saint-Martory, C., Theunis, J., Bensafi-Benaouda, A., Degouy, A., Schmitt, A.M., and Redoulès, D. Association between collagen production and mechanical stretching in dermal extracellular matrix: in vivo effect of cross-linked hyaluronic acid filler. A randomised, placebo-controlled study. J Dermatol Sci **69,** 187, 2013.
12. Wohlrab, J., Wohlrab, D., and Neubert, R.H. Comparison of noncross-linked and cross-linked hyaluronic acid with

regard to efficacy of the proliferative activity of cutaneous fibroblasts and keratinocytes in vitro. J Cosmet Dermatol **12,** 36, 2013.
13. Bencherif, S.A., Sands, R.W., Bhatta, D., Arany, P., Verbeke, C.S., Edwards, D.A., and Mooney, D.J. Injectable preformed scaffolds with shape-memory properties. Proc Natl Acad Sci U S A **109,** 19590, 2012.
14. Koshy, S.T., Ferrante, T.C., Lewin, S.A., and Mooney, D.J. Injectable, porous, and cell-responsive gelatin cryogels. Biomaterials **35,** 2477, 2014.
15. Béduer, A., Braschler, T., Peric, O., Fantner, G.E., Mosser, S., Fraering, P.C., Benchérif, S., Mooney, D.J., and Renaud, P. A compressible scaffold for minimally invasive delivery of large intact neuronal networks. Adv Healthc Mater **28,** 301, 2015.
16. Klinger, M., Caviggioli, F., Klinger, F.M., Giannasi, S., Bandi, V., Banzatti, B., Forcellini, D., Maione, L., Catania, B., and Vinci, V. Autologous fat graft in scar treatment. J Craniofac Surg **24,** 1610, 2013.
17. Yun, I.S., Jeon, Y.R., Lee, W.J., Lee, J.W., Rah, D.K., Tark, K.C., and Lew, D.H. Effect of human adipose derived stem cells on scar formation and remodeling in a pig model: a pilot study. Dermatol Surg **38,** 1678, 2012.
18. Heit, Y.I., Lancerotto, L., Mesteri, I., Ackermann, M., Navarrete, M.F., Nguyen, C.T., Mukundan, S., Jr., Konerding, M.A., Del Vecchio, D.A., and Orgill, D.P. External volume expansion increases subcutaneous thickness, cell proliferation, and vascular remodeling in a murine model. Plast Reconstr Surg **130,** 541, 2012.
19. Lancerotto, L., Chin, M.S., Freniere, B., Lujan-Hernandez, J.R., Li, Q., Valderrama Vasquez, A., Bassetto, F., Del Vecchio, D.A., Lalikos, J.F., and Orgill, D.P. Mechanisms of action of external volume expansion devices. Plast Reconstr Surg **132,** 569, 2013.
20. Rubert, M., Alonso-Sande, M., Monjo, M., and Ramis, J.M. Evaluation of alginate and hyaluronic acid for their use in bone tissue engineering. Biointerphases **7,** 11, 2012.
21. Kissin, E.Y., Schiller, A.M., Gelbard, R.B., Anderson, J.J., Falanga, V., Simms, R.W., Korn, J.H., and Merkel, P.A. Durometry for the assessment of skin disease in systemic sclerosis. Arthritis Rheumat **55,** 603, 2006.
22. Falanga, V., and Bucalo, B. Use of a durometer to assess skin hardness. J Am Acad Dermatol **29,** 47, 1993.
23. Reisfeld, P.L. A hard subject: use of a durometer to assess skin hardness. J Am Acad Dermatol **31,** 515, 1994.
24. Wolff, E., Pal, L., Altun, T., Madankumar, R., Freeman, R., Amin, H., Harman, M., Santoro, N., and Taylor, H.S. Skin wrinkles and rigidity in early postmenopausal women vary by race/ethnicity: baseline characteristics of the skin ancillary study of the keeps trial. Fertil Steril **95,** 658, 2011.
25. Moon, K.W., Song, R., Kim, J.H., Lee, E.Y., Lee, E.B., and Song, Y.W. The correlation between durometer score and modified Rodnan skin score in systemic sclerosis. Rheumatol Int **32,** 2465, 2012.
26. Yannas, I.V., Lee, E., Orgill, D.P., Skrabut, E.M., and Murphy, G.F. Synthesis and characterization of a model extracellular matrix that induces partial regeneration of adult mammalian skin. Proc Natl Acad Sci U S A **86,** 933, 1989.
27. O'Brien, F.J., Harley, B.A., Yannas, I.V., and Gibson, L.J. The effect of pore size on cell adhesion in collagen-GAG scaffolds. Biomaterials **26,** 433, 2005.
28. Weinberg, M.J., and Solish, N. Complications of hyaluronic acid fillers. Facial Plast Surg **25,** 324, 2009.
29. Park, T.H., Seo, S.W., Kim, J.K., and Chang, C.H. Clinical outcome in a series of 173 cases of foreign body granuloma: improved outcomes with a novel surgical technique. J Plast Reconstr Aesthet Surg **65,** 29, 2012.
30. Park, T.H., Seo, S.W., Kim, J.K., and Chang, C.H. Clinical experience with hyaluronic acid-filler complications. J Plast Reconstr Aesthet Surg **64,** 892, 2011.
31. Alijotas-Reig, J., Hindie, M., Kandhaya-Pillai, R., and Miro-Mur, F. Bioengineered hyaluronic acid elicited a nonantigenic T cell activation: implications from cosmetic medicine and surgery to nanomedicine. J Biomed Mater Res Part A **95,** 180, 2010.
32. Kassir, R., Kolluru, A., and Kassir, M. Extensive necrosis after injection of hyaluronic acid filler: case report and review of the literature. J Cosmet Dermatol **10,** 224, 2011.
33. Beleznay, K., Carruthers, J.D., Humphrey, S., and Jones, D. Avoiding and treating blindness from fillers: a review of the world literature. Dermatol Surg **41,** 1097, 2015.
34. Kim, W.B., and Alhusayen, R.O. Skin necrosis from intra-articular hyaluronic acid injection. J Cutan Med Surg **19,** 182, 2015.
35. Carruthers, J.D., Fagien, S., Rohrich, R.J., Weinkle, S., and Carruthers, A. Blindness caused by cosmetic filler injection: a review of cause and therapy. Plast Reconstr Surg **134,** 1197, 2014.

Address correspondence to:
Christoph S. Nabzdyk, MD
Department of Anesthesiology,
Perioperative and Pain Medicine
Brigham and Women's Hospital
Harvard Medical School
CWN-L1, Room L111
75 Francis Street
Boston, MA 02115

E-mail: cnabzdyk@partners.org

Received: June 29, 2016
Accepted: November 9, 2016
Online Publication Date: January 2, 2017